Journal of Iron and Steel Research, International 24 (2017) 579−585

Contents lists available at ScienceDirect

Journal of Iron and Steel Research, International

journal homepage: www.chinamet.cn

Effect of slag composition on steel cleanliness in interstitial-free steel

Rui Wang[1], Yan-ping Bao[1,*], Yi-hong Li[2], Tai-quan Li[3], Di Chen[3]

[1] State Key Laboratory of Advanced Metallurgy, University of Science and Technology Beijing, Beijing 100083, China

[2] School of Materials Science and Engineering, Taiyuan University of Science and Technology, Taiyuan 030024, Shanxi, China

[3] Handan Iron & Steel Group Co., Ltd. of HBIS, Handan 056000, Hebei, China

ARTICLE INFO

Key words:
IF steel
Ladle slag
Reoxidation
Inclusion
Holding process

ABSTRACT

Ladle slag affects steel cleanliness at the end of the Ruhrstahl-Hereaeus (RH) and holding process. The relationship between composition of ladle slag, total oxygen (TO) and inclusions was investigated using X-ray fluorescence (XRF), infrared absorption, and SEM+EDS methods. The results indicate that TO in steel at the end of RH increases linearly with increasing FeO content in slag. TO is lower when w_{CaO}/w_{Al2O3} (C/A)=1.5−2.0 than that of C/A=1.0−1.4 under an approximate content of FeO. During the holding process, irregular Al_2O_3 inclusions are newly generated due to slag reoxidation. Additionally, Al_2O_3-Ti_xO inclusions are newly generated in the steel when the content of FeO is higher. By combining experimental and thermodynamic calculation results, it is determined that the slag has a good melting property within the zone of C/A=1.2−1.8 and adsorption capacity of Al_2O_3 when the content of SiO_2 in slag is controlled at 4%−6%. The increase in the C/A ratio and the decrease of FeO content in slag can slow down the reoxidation rate.

Symbol List

R_d—Absorption capacity of slag;
K—Mass transfer coefficient related to melting point, $\mu m \cdot s^{-1}$;
C_s—Saturation fraction of Al_2O_3 in slag, wt. %;
C_b—Real mass fraction of Al_2O_3 in slag, wt. %;
J_S—Diffusion flux of FeO in slag, $mol \cdot cm^{-2} \cdot s^{-1}$;
J_M—Diffusion flux of FeO in steel, $mol \cdot cm^{-2} \cdot s^{-1}$;
k_S—Mass transfer coefficient of FeO in slag, $cm \cdot s^{-1}$;
k_M—Mass transfer coefficient of FeO in steel, $cm \cdot s^{-1}$;
$c(FeO)$—Concentration of FeO in slag, $mol \cdot cm^{-3}$;
$c(FeO)^i$—Concentration of FeO at steel/slag interface, $mol \cdot cm^{-3}$;
$c[O]$—Concentration of [O] in steel, $mol \cdot cm^{-3}$;
$c[O]^i$—Concentration of [O] at steel/slag interface, $mol \cdot cm^{-3}$.

1. Introduction

In recent years, with the development of automobile industry, the growth of market demand for high quality steel for deep drawing is predictable. Due to excellent deep drawability, interstitial-free (IF) steel is widely used in automobile industry[1,2]. However, silver defects in cold sheets often emerge. Several studies[3-5] have shown that large Al_2O_3 inclusions and mold slags entrapped in steel are the main reasons for the formation of defects.

The general process of producing IF steel is as follows: BOF (basic oxygen furnace)→RH (Ruhrstahl-Hereaeus)→Holding process→CC (continuous casting). Thus, some converter slag with a high FeO content enters into the ladle during tapping. This slag accompanies steel in ladle during the RH and holding process, and steel becomes contaminated with oxidizing slag if ladle slag is not modified. In Nippon Steel, the TFe (total Fe) content of ladle slag is reduced below 4% by adding a modifier after tapping in IF steel, and the surface defects of cold-rolled sheets are reduced by 1/6 compared with a conventional process[6]. From the testing results of NKK (Nippon Kokan), the index of surface defects is decreased by 80% after deoxidizing of ladle slag[7]. The study by Sun and Mori[8] showed that more alumina inclusions were generated in the metal bath for slag with a higher FeO or MnO content and metal with a lower aluminum content and the restrictive step of

* Corresponding author. Prof., Ph.D.
E-mail address: *baoyp@ustb.edu.cn* (*Y. P. Bao*).

Received 21 September 2016; Received in revised form 11 December 2016; Accepted 15 December 2016
Available online 15 June 2017

reoxidation of $[Al]_s$ is the diffusion of $[Al]_s$ in steel or diffusion of (FeO) in slag. Lee et al.[9] found that the reoxidation rate increased linearly with increasing TFe content in the case of TFe content higher than 1.5 wt.%, and it decreased with increasing the $w_{CaO}/w_{Al_2O_3}$ (C/A) ratio of the slag for a given TFe content.

The modification of ladle slag was performed not only to decrease the content of FeO but also to control the proper ratio of C/A to ensure the absorption capacity of Al_2O_3. Yoon et al.[10] found that controlling the C/A ratio is the most efficient method for removing inclusions from bearing steels, and its value was most effective at 1.7－1.8. The total oxygen (TO) can be reduced from $(10－12)\times10^{-6}$ to $(5－8)\times10^{-6}$. However, the content of FeO was very low in refining slag during bearing steel production. In Kawasaki Steel[11], through the modification of slag in ultra-low carbon steel production, it was found that slag had good absorption capacity of Al_2O_3 by controlling the C/A ratio from 1.2 to 1.8.

All above-mentioned studies showed that the control over the content of FeO and C/A ratio is the key during the production. However, there is a lack of theoretical description to explain why the steel cleanliness is improved by controlling slag composition. Additionally, the content of SiO_2 is not mentioned in any of the above-mentioned studies, but it affects the melting property and absorption capacity of Al_2O_3. In this paper, the effect of the content of SiO_2 and FeO as well as C/A ratio on steel cleanliness and steel reoxidation was investigated.

2. Production Process and Experimental Method

2.1. Production process

The process adopted to produce IF steel is as follows: 280 t BOF → RH → Holding process → CC. During tapping, an amount of lime is added into the ladle, and slag deoxidant is added onto the slag. The RH vacuum treatment includes decarburization, followed by aluminum deoxidation, then Ti-Fe alloying and keeping the RH circulation time for 8 min. After the RH treatment, molten steel remains unstirred in the ladle for 30－40 min before casting.

2.2. Experimental method

In total, 10 experimental heats were carried out. The difference between the two processes was the amount of deoxidant addition. In Process A, the added amount was more than that in Process B. The addition of lime during tapping of different heats is shown in Table 1. Slag and steel samples were collected at the end of the RH process of each heat. For Heat 2, Heat 3, Heat 4, and Heat 6, steel samples were collected at 5, 10, and 15 min of holding time.

Table 1
Addition of lime for each experiment

Process	Heat No.	CaO/kg
A	1	800
	2	800
	3	500
	4	500
	5	500
B	6	800
	7	800
	8	800
	9	500
	10	500

The initial oxygen activities before deoxidation of ten experimental heats were measured.

The total oxygen content of steel samples was analyzed using the infrared absorption method. Steel composition was analyzed via the ICP-AES method. Slag composition was analyzed using an X-ray fluorescence spectrometer. The characterization of inclusions was observed and analyzed using scanning electron microscopy (SEM) and an energy-dispersive X-ray spectrometer (EDS). The samples from two heats were observed at 100 locations with 3000 times magnification using SEM to obtain the inclusion type, quantity, and size.

3. Results and Discussion

3.1. Steel and slag compositions

Table 2 shows the slag composition of 10 heats. The content of FeO in Process A is lower than that in Process B, and the ratio of C/A varies due to different amouts of lime addition. TFe (Fe^{2+} and Fe^{3+}) and SiO_2 are main reducible oxides, and TFe can be treated as FeO[12].

The content of MgO is steadily controlled at approximately 5%. However, the content of SiO_2 fluctuates from 2% to 9%, and the effect of SiO_2 content on slag property will be discussed in the following section.

Table 3 provides steel composition at the end of RH

Table 2
Slag composition in each heat (wt.%)

Heat No.	CaO	FeO	SiO_2	MgO	MnO	Al_2O_3	C/A
1	40.0	15.9	4.1	5.1	2.1	26.3	1.5
2	42.3	13.5	7.2	5.0	2.4	27.6	1.5
3	34.7	13.5	3.1	4.9	2.9	35.9	1.0
4	38.2	13.5	6.1	4.6	2.5	32.1	1.2
5	39.3	14.8	6.3	4.6	2.6	32.1	1.2
6	37.9	24.9	2.7	5.7	2.4	21.9	1.7
7	41.1	20.1	4.9	4.1	2.2	19.6	2.0
8	39.8	21.1	8.6	4.6	2.0	21.1	1.9
9	36.3	19.8	3.4	5.0	2.2	28.9	1.3
10	36.4	18.1	4.9	4.2	2.8	29.1	1.3

Table 3
Steel composition in each heat (wt.%)

Heat No.	C	Si	Mn	P	S	$[Al]_s$	Ti
1	0.0010	0.0021	0.12	0.0110	0.0070	0.044	0.074
2	0.0012	0.0018	0.10	0.0099	0.0091	0.041	0.073
3	0.0012	0.0021	0.11	0.0080	0.0050	0.039	0.075
4	0.0011	0.0023	0.11	0.0099	0.0073	0.040	0.074
5	0.0010	0.0020	0.12	0.0070	0.0040	0.043	0.079
6	0.0010	0.0020	0.11	0.0070	0.0050	0.040	0.072
7	0.0011	0.0023	0.12	0.0082	0.0065	0.041	0.075
8	0.0012	0.0020	0.11	0.0098	0.0072	0.047	0.077
9	0.0010	0.0020	0.11	0.0090	0.0070	0.048	0.079
10	0.0011	0.0018	0.11	0.0071	0.0061	0.043	0.070

process for 10 heats. Steel composition of 10 heats is stably controlled. The content of $[Al]_s$ in steel is from 0.039% to 0.048%, and the concentration of [Ti] is from 0.070% to 0.079%.

Table 4 shows that the initial oxygen activity during most experiments is between 400×10^{-6} and 450×10^{-6}. The addition of Al particles (10－20 mm) is also shown in Table 4. Thus, the quantity of inclusions due to deoxidation is close to each other.

Table 4
Initial oxygen activity before deoxidation

Heat No.	Initial oxygen activity before deoxidation/10^{-6}	Addition of Al/kg
1	420.1	370
2	443.8	378
3	440.6	380
4	460.8	390
5	454.8	398
6	390.9	358
7	451.7	385
8	439.8	383
9	426.3	385
10	409.4	384

3.2. Total oxygen in steel

Fig. 1 shows that the TO in steel at the end of RH increases linearly with increasing FeO content in slag. The TO is lower when C/A＝1.5－2.0 than when C/A＝1.0－1.4 under an approximate content of FeO.

In Fig. 2, the FeO content and initial TO of Heat 2 and Heat 4 are approximate at the beginning of holding, but the variation of TO in two heats is distinct due to different C/A ratios of slag. The TO of Heat 2 with C/A＝1.5 is mainly unchanged with the increase in holding time, and TO of Heat 4 with C/A＝1.2 clearly increases within 10 min of holding time. After holding for 15 min, the TO of Heat 4 is significantly higher than that of Heat 2. In general, steel has a smaller oxygen potential than slag, and oxygen is transferred from slag to the molten steel,

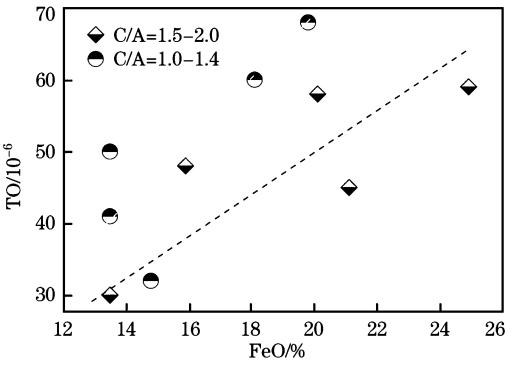

Fig. 1. Effects of FeO content and C/A ratio on total oxygen at the end of RH.

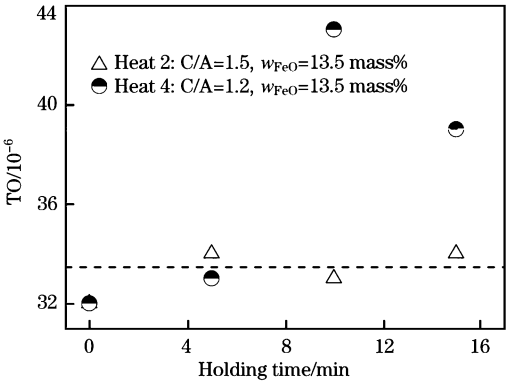

Fig. 2. Change in total oxygen of Heat 2 and Heat 4.

leading to the reoxidation of steel and formation of inclusions. Meanwhile, inclusions are removed by floating from the molten steel followed by absorption by slag. Then, TO remains unchanged when a balance between the reoxidation and inclusion removal rates is achieved[13]. Thus, a balance is reached between the reoxidation and inclusion removal rates of Heat 2, while the reoxidation rate is greater than the inclusion removal rate of Heat 4 due to the lower C/A ratio.

Fig. 3 indicates that the TO of Heat 6 decreases gradually, and at the holding time of 15 min it is close to that of Heat 3 of which the initial TO was lower than 10×10^{-6}. The TO of Heat 3 decreases within 5 min and then remains unchanged. With the inclusions removed, the removal rate of inclusions is decreased. However, a low C/A causes poor absorptivity

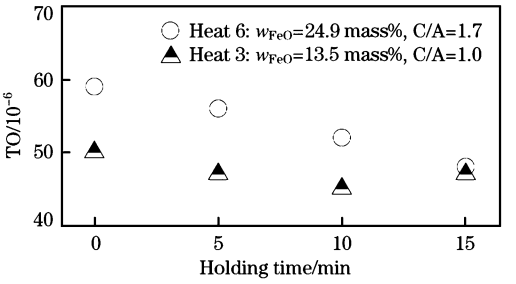

Fig. 3. Change in total oxygen of Heat 3 and Heat 6.

of slag in Heat 3. These two reasons cause the change of TO in Heat 3.

Several studies[14,15] have shown that in a CaO-Al_2O_3-SiO_2 system, the increase in C/A ratio can accelerate the dissolution of Al_2O_3 inclusion in slag, and the increase in C/A ratio results in an increase in interfacial energy and decrease in wettability between slag and Al_2O_3 inclusion, which accounts for the TO change in Figs. 1－3.

3.3. Inclusions in steel

Fig. 4 shows the typical inclusions of Al_2O_3 at the holding time of 15 min. In Processes A and B, those are Al_2O_3 clusters in Fig. 4(a) due to aggregation of spherical inclusions, stick inclusion in Fig. 4(b) and petal inclusions in Fig. 4(c). Because of the interfacial tension effect, Al_2O_3 inclusions transform from irregular shapes (stick-like, spherical, petal-shaped, and dendritic) into the spherical shape[16]. However, stick-like and dendritic inclusions appear during the holding process, which accounts for the stick-like inclusions. Dendritic inclusions are newly generated and are not derived from collision and aggregation. Yoon et al.[10] illustrates that supersaturation of [O] or $[Al]_s$ leads to the generation of stick-like and dendritic inclusions of Al_2O_3. However, during the holding process, the $[Al]_s$ content in steel does not significantly change. Thus, the only supersaturation of [O], derived from (FeO) in slag, results in the generation of stick-like and dendritic inclusions. As shown in Figs. 5 and 6, many Al_2O_3-Ti_xO inclusions appear during the Process B. These inclusions

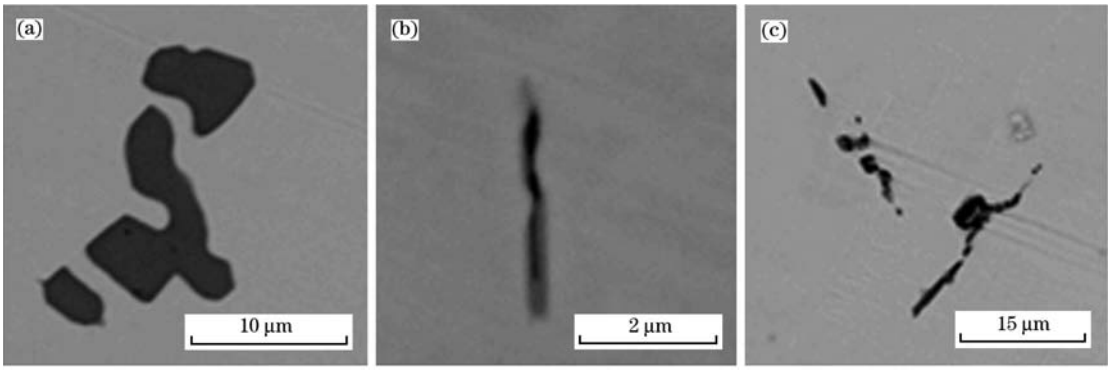

Fig. 4. Typical inclusions of Al_2O_3 for holding time of 15 min in Processes A and B.

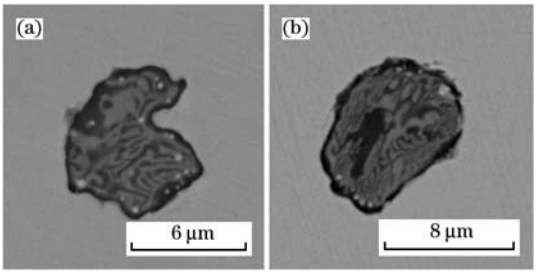

Fig. 5. Al_2O_3-Ti_xO inclusions at holding time of 15 min in Process B.

are newly generated during the holding process. According to Refs. [17] and [18], Al_2O_3-Ti_xO is generated due to the high concentration of [Ti] or [O]. With the addition of the Ti-Fe alloy into steel, Al_2O_3-Ti_xO inclusions can form at the local high titanium concentration region before steel is completely mixed. Once the composition of steel is uniform via the RH circulation, the only predicted thermodynamically stable phase is Al_2O_3 for the IF steel composition. This is consistent with the results in Ref. [19]. Thus, the Al_2O_3-Ti_xO inclusions form because of the high [O] concentration rather than [Ti] due to slag reoxidation. The inclusions due to reoxidation are generated in both Process A and Process B. The phase stability diagrams of [Ti] and $[Al]_s$ content in steel at 1873 K are calculated using FactSage 7.0 and are shown in Fig. 7. Due to reoxidation, the generation of Al_2O_3 inclusion leads to the decrease of local $[Al]_s$ content. Then, the local [O] content in Process A is not sufficient for the generation of Al_2O_3-Ti_xO inclusion. However, the higher [O] content due to the higher (FeO) content in Process B is enough for the inclusion generation.

Figs. 8 and 9 show the changes in size and quantity of inclusion during the holding process in Heat 2 and Heat 4, respectively. The quantity of inclusions in Heat 2 decreases gradually during the holding process, and the inclusions with sizes above 10 μm float up within 15 min. The size of most inclusions in steel is between 1 and 5 μm. The quantity of inclusions in Heat 4 clearly increases at the holding time of 5 to 10 min, and most 1 μm inclusions are newly generated at the holding time of 10 min. This indicates that reoxidation occurs during the holding process. The change in inclusion quantity in Heats 2 and 4 is consistent with the change in TO.

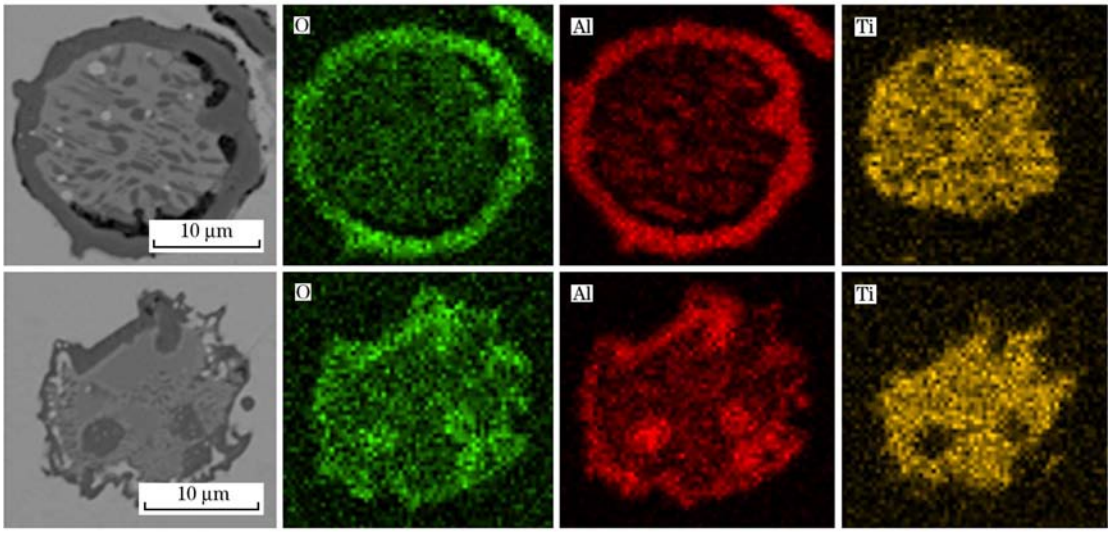

Fig. 6. Typical morphologies of Al_2O_3-Ti_xO in Process B.

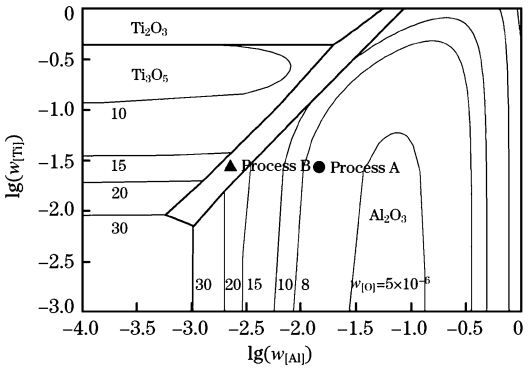

Fig. 7. Fe-Al-Ti-O phase diagram from FactSage 7.0.

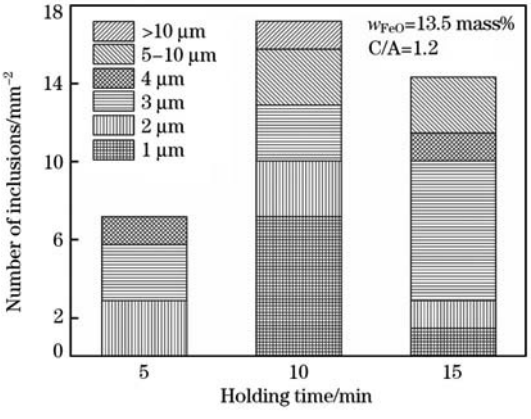

Fig. 8. Change in Al_2O_3 inclusions during holding process in Heat 2.

3.4. Effect of SiO_2 content in slag on absorption capacity for Al_2O_3

According to Ref. [11], absorption capacity is better when the ratio of C/A＝1.2－1.8. In Fig. 10, with increasing SiO_2 content, the low melting point area when the FeO content is below 25% gradually moves

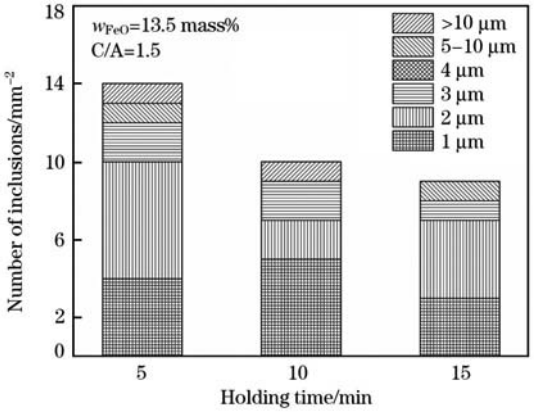

Fig. 9. Change in Al_2O_3 inclusions during holding process in Heat 4.

to the phase diagram zone where C/A＝1.2－1.8. When the SiO_2 content is 10%, the area is still in the zone of C/A＝1.2－1.8 even when the content of FeO is less than 5%.

Fig. 11 shows the Al_2O_3 saturation level in slag at different SiO_2 contents. The addition of Al_2O_3 in the horizontal ordinate simulates the accumulation of Al_2O_3 with time. The figure suggests that with decreasing SiO_2 content, the Al_2O_3 saturation level in slag increases, and the time of the starting solution of Al_2O_3 shortens.

Based on Figs. 10 and 11, it is possible to conclude that the area of low melting point gradually deviates from the zone of C/A＝1.2－1.8. However, the absorption capacity for Al_2O_3 increases when the content of SiO_2 decreases. The rate of Al_2O_3 dissolution in slag can be calculated using Eq. (1). The large saturated mass fraction is conducive for accelerating the dissolution rate. Thus, when the SiO_2 content is controlled from 4% to 6%, the slag has a good melting

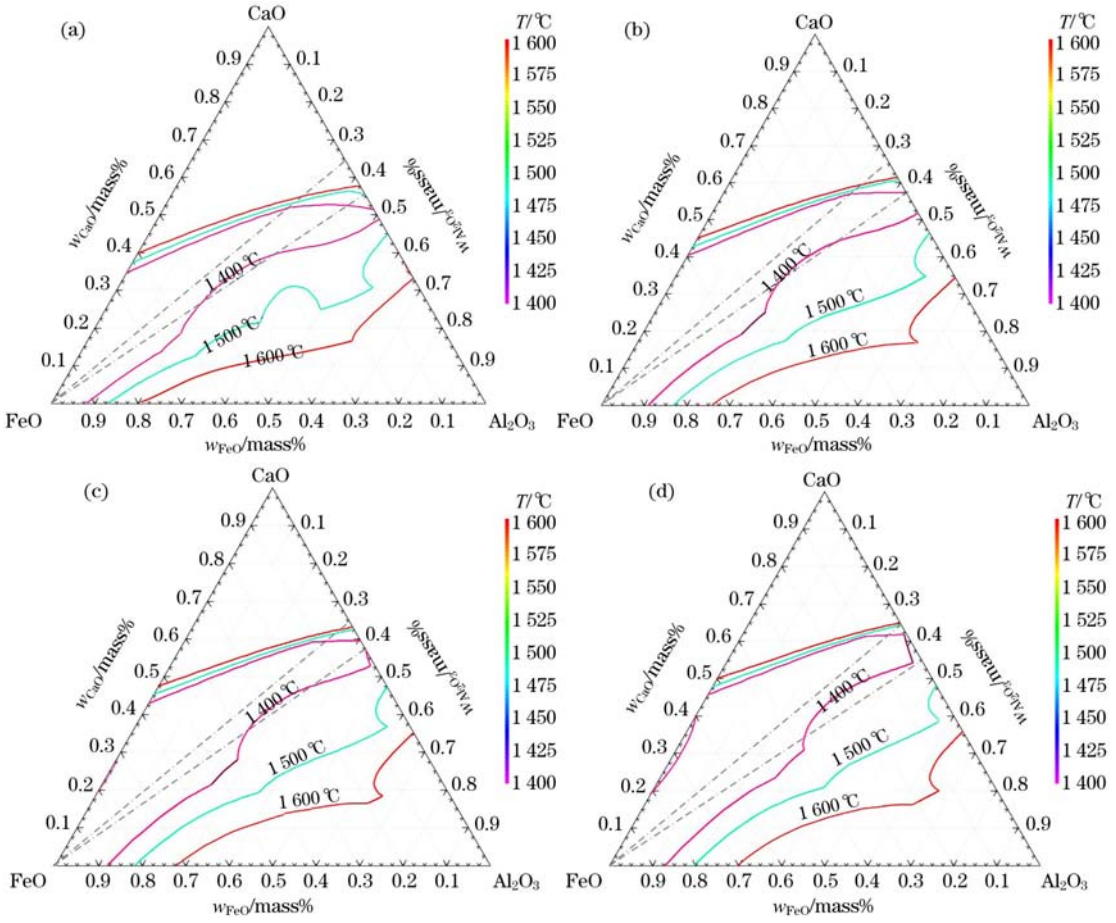

(a) SiO_2=2%; (b) SiO_2=4%; (c) SiO_2=6%; (d) SiO_2=10%.

Fig. 10. Variation of low melting point area at different contents of SiO_2.

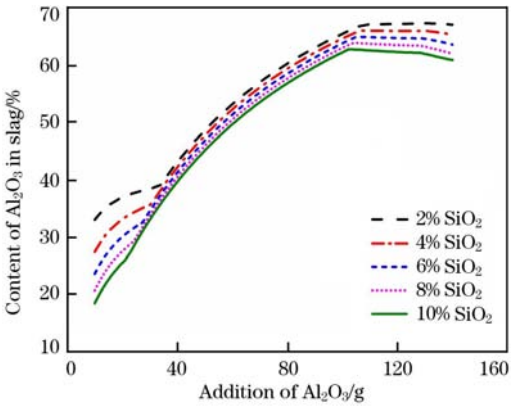

Fig. 11. Al_2O_3 saturation level in slag at different SiO_2 contents.

property in the zone of C/A=1.2-1.8 and a better adsorption capacity for Al_2O_3.

$$R_d = K(C_s - C_b) \quad (1)$$

3.5. *Effect of FeO on steel reoxidation*

Wang et al.[20] found that there are two mechanisms that explain reoxidation.

(1) Reoxidation reaction at the slag/steel interface

$$2[Al]+3(FeO)=(Al_2O_3)+3[Fe] \quad (2)$$

(2) Reoxidation reaction in the steel interior

$$(FeO)=[Fe]+[O] \quad (3)$$

$$2[Al]+3[O]=(Al_2O_3) \quad (4)$$

$$4[O]+2[Al]+x\,Ti=Al_2O_3\text{-}Ti_xO \quad (5)$$

Newly generated Al_2O_3 and Al_2O_3-Ti_xO inclusions are found during the holding process. This suggests that reoxidation occurs in the steel interior. The reaction of slag and steel can be described via the two-film theory, as shown in Fig. 12.

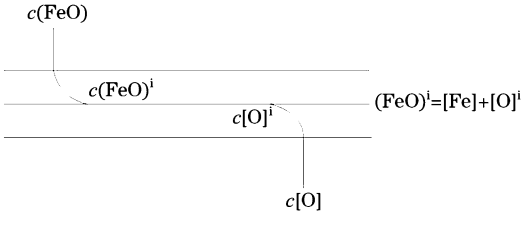

Fig. 12. Schematic diagram of two-film theory of slag/steel reaction.

The step of slag reoxidation to steel is shown as follows.

(1) (FeO) in slag diffused to the slag/steel interface:

$$J_s = k_s[c(FeO)-c(FeO)^i] \quad (6)$$

(2) The decomposition reaction of (FeO) occurs at the interface:

$$(FeO)^i=[Fe]+[O]^i \quad (7)$$

$$K=\frac{a[O]^i}{a(FeO)^i} \quad (8)$$

(3) $[O]^i$ at the interface is transferred into steel:

$$J_M=k_M[c[O]^i-c[O]] \quad (9)$$

To reduce the rate of slag reoxidation into steel, the diffusion rate of $[O]^i$ at the slag-steel interface on the steel side should be reduced by reducing the [O] content. It can be easily shown from Eqs. (7) and (8) that the activity of (FeO) is available to be reduced for reducing the [O] content. The activity of (FeO) decreases with the decrease of the (FeO) content in slag. Thus, by decreasing the (FeO) content of slag, the reoxidation to steel can be decreased.

Lee et al.[9] found that when TFe>1.5 wt.%, the value of $k_{[Al]}$ increases with increasing TFe content for a given C/A mass ratio. For a given TFe content, $k_{[Al]}$ decreases with increasing value of the C/A ratio. $k_{[Al]}$ represents the decreasing rate of the soluble aluminum content in the molten steel that is in contact with slag. The value of $k_{[Al]}$ can be considered as a measurement of reoxidation potential and oxidizing tendency of the slag.

All studies show that the increase in C/A ratio promotes slag to absorb Al_2O_3 inclusion, and also simultaneously reduces the reoxidation rate of slag to steel. This is in agreement with the TO change in Figs. 1−3.

4. Conclusions

(1) The TO in steel at the end of RH increases linearly with the increase of FeO content in slag. TO is lower when C/A=1.5−2.0 than when C/A=1.0−1.4 under an approximate content of FeO.

(2) During the holding process, some irregular Al_2O_3 inclusions (stick-like and dendritic shapes) are found in steel, and newly generated Al_2O_3-Ti_xO inclusions occur in heating experiments with a high FeO content.

(3) The content of SiO_2 in slag influences the change of low melting point area and absorption capacity of Al_2O_3. By controlling the SiO_2 content at 4%−6%, the slag had a good melting property within the range of C/A=1.2−1.8 and adsorption capacity for Al_2O_3.

(4) The increasing C/A ratio and decreasing FeO content in slag slows down the reoxidation rate.

Acknowledgment

This work was financially supported by National Natural Science Foundation of China (Nos. 51574019 and 51404018), the National Key Technology R&D Program (2015BAF30B1), and Ph. D. Early Development Program of Taiyuan University of Science and Technology (No. 20152008).

References

[1] Y. Q. Feng, F. M. Wang, S. L. Tao, D. Q. Zhao, X. Y. Zhang, J. Iron Steel Res. Int. 20 (2013) No. 5, 42-49.
[2] B. Yan, S. H. Jiao, D. H. Zhang, J. Iron Steel Res. Int. 23 (2016) 160-165.
[3] M. Takashi, M. Morishita, H. Nakata, M. Kokita, ISIJ Int. 46 (2006) 1817-1822.
[4] H. Yasunak, R. Yamana, T. Inoue, T. Saito, Tetsu-to-Hagane 81 (1995) 529-534.
[5] H. Cui, H. J. Wu, F. Yue, W. S. Wu, M. Wang, Y. P. Bao, B. Chen, C. X. Ji, J. Iron Steel Res. Int. 18 (2011) Suppl. 1, 335-340.
[6] K. Tanizawa, F. Yamaguchi, K. Inaoka, Metall. Ital. 84 (1992) No. 1, 17-22.
[7] A. Kamesui, CAMP-ISIJ 5 (1992) No. 4, 1288.
[8] H. P. Sun, K. Mori, ISIJ Int. 36 (1996) Suppl. 1, 34-37.
[9] K. Y. Lee, J. M. Park, C. W. Park, in: VII International Conference on Molten Slags Fluxes and Salts, The South African Institute of Mining and Metallurgy, Johannesburg, 2004, pp. 601-606.
[10] B. H. Yoon, K. H. Heo, J. S. Sohn, Ironmak. Steelmak. 29 (2002) 215-218.
[11] T. Ehara, Y. Kurose, T. Fujimura, J. Hasunuma, R. Asaho, in: 1996 Steelmaking Conference Proceedings, Iron and Steel Society, Warrendale, Pittsburgh, 1996, pp. 485-486.
[12] Y. Taniguchi, K. Motita, N. Sano, ISIJ Int. 37 (1997) 956-961.
[13] H. Goto, K. Miyazawa, ISIJ Int. 38 (1998) 256-259.
[14] M. Valdez, G. Shannon, S. Sridhar, ISIJ Int. 46 (2006) 450-457.
[15] J. Choi, H. Lee, ISIJ Int. 43 (2003) 1348-1355.
[16] W. Yang, X. H. Wang, L. F. Zhang, W. J. Wang, Steel Res. Int. 84 (2013) 878-891.
[17] D. C. Park, I. H. Jung, C. H. Rhee, H. G. Lee, ISIJ Int. 44 (2004) 1669-1678.
[18] W. C. Doo, D. Y. Kim, S. C. Kang, K. W. Yi, Met. Mater. Int. 13 (2007) 249-255.
[19] Y. M. Qin, X. H. Wang, F. X. Huang, B. Chen, C. X. Chen, Metall. Res. Technol. 112 (2015) No. 4, 405.
[20] M. Wang, Y. P. Bao, H. Cui, W. S. Wu, H. J. Wu, J. Univ. Sci. Technol. Beijing 32 (2010) 432-437 (in Chinese).